Progress in Oceanography 131 (2015) 146–158

Contents lists available at ScienceDirect

Progress in Oceanography

journal homepage: www.elsevier.com/locate/pocean

Potential habitat for chum salmon (*Oncorhynchus keta*) in the Western Arctic based on a bioenergetics model coupled with a three-dimensional lower trophic ecosystem model

Seokjin Yoon [a,*], Eiji Watanabe [b], Hiromichi Ueno [a,c], Michio J. Kishi [a,c]

[a] Faculty of Fisheries Sciences, Hokkaido University, N10 W5, Kita-ku, Sapporo, Hokkaido 060-0810, Japan
[b] Japan Agency for Marine-Earth Science and Technology, 2-15 Natsushima, Yokosuka, Kanagawa 237-0061, Japan
[c] Graduate School of Environmental Science, Hokkaido University, N10 W5, Kita-ku, Sapporo, Hokkaido 060-0810, Japan

ARTICLE INFO

Article history:
Received 27 August 2014
Received in revised form 10 December 2014
Accepted 10 December 2014
Available online 19 December 2014

ABSTRACT

Chum salmon (*Oncorhynchus keta*) are predominantly located in the Bering Sea during summer and fall. However, several studies have recently reported a different tendency as follows. Observed densities of chum salmon were higher in the vicinity of the Bering Strait and the Chukchi Sea than the eastern Bering Sea in September 2007, and Japanese chum salmon migrated to northern areas in the Bering Sea during summer 2009. The sea surface temperature (SST) in the Arctic marginal seas has increased since the mid-1960s, and especially since 2000. We speculated that the SST increase directly promoted salmon northing from the Bering Sea to the Western Arctic. In this study, we estimated the potential habitat for chum salmon in the Western Arctic using a bioenergetics model coupled with a three-dimensional lower trophic ecosystem model (3-D NEMURO). "Potential habitat" was defined as "an area where chum salmon could grow (i.e., the growth rate was positive)". In the bioenergetics model, the growth rate of an individual chum salmon was calculated as a function of water temperature, salinity, and prey density, which were obtained from the 3-D NEMURO model results. To evaluate the habitat responses under a global warming scenario, we used the modeled monthly change of water temperature between 2005 (averaged from 2001 to 2010) and 2095 (averaged from 2091 to 2100) under the IPCC SRES-A1B scenario. Our calculations, following the global warming scenario, suggested that the potential habitat for chum salmon would expand to the north due to the increase in water temperature and prey density. In contrast, south of 71°N during summer, the potential habitat would shrink regionally because the water temperature exceeded the optimal condition.

Introduction

Chum salmon (*Oncorhynchus keta*) are distributed widely in the North Pacific, and represent an important commercial fishery resource for North Pacific countries. Determining the distribution and origins of chum salmon will provide valuable information to help clarify stock-specific patterns of ocean migration for stock assessment (Sato et al., 2009b). Chum salmon are predominantly located in the Bering Sea during summer and fall (Sato et al., 2009a; Urawa et al., 2009). However, several studies have recently reported a different tendency. The observed densities of chum salmon were higher in the vicinity of the Bering Strait and the Chukchi Sea than the eastern Bering Sea in September 2007 (Moss et al., 2009), and Japanese stocks migrated to northern areas (>60°N) in the Bering Sea during summer 2009 (Sato et al., 2012).

Global warming has affected the growth and survival of Asian chum salmon since the 1990s; and in the near future (~2095), a shrinking of suitable habitat for chum salmon in the North Pacific and a northward shift in distribution into the Chukchi Sea have been projected under the Special Report on Emissions Scenarios (SRES) A1B of the Intergovernmental Panel on Climate Change (IPCC) (Kaeriyama, 2008). Fig. 1 shows the current sea surface temperature (SST) in the Bering Sea, obtained from the World Ocean Atlas 2005 (Locarnini et al., 2006), and the projected SST in 2095 (averaged from 2091 to 2100) simulated under a global warming scenario (SRES A1B) (Kawamiya et al., 2005). The optimal temperature for the growth and feeding of chum salmon ranges from 8 °C to 12 °C, and the adaptable temperature for available habitats ranges from 5 °C to 13 °C (Kaeriyama et al., 2012). In the Bering Sea, the SST is at the optimal temperature under current conditions, whereas the SST exceeds the optimum temperature during

* Corresponding author at: Fisheries and Environmental Oceanography, Field Science Education and Research Center, Kyoto University, Oiwake-cho, Kitasirakawa, Sakyo-ku, Kyoto 606-8502, Japan. Tel./fax: +81 75 753 6468.
E-mail address: seokjin.yoon@gmail.com (S. Yoon).

http://dx.doi.org/10.1016/j.pocean.2014.12.009
0079-6611/

summer under the global warming scenario (SRES A1B). The SST in the Arctic marginal seas has increased since the mid-1960s, and especially since 2000 (Steele et al., 2008), and we speculate that northerly distribution will expand with global warming. The SST increase has directly affected the northerly extent of current chum salmon distribution, and the northward migration would accelerate with global warming. Therefore, we focused on chum salmon migrating northward to the Western Arctic during summer and fall.

Numerical modeling is one of the most powerful tools used to estimate the impacts of global warming on marine ecosystems (Harley et al., 2006; Yoon et al., 2013). Bioenergetics models of chum salmon have been used to investigate the relationship between environmental conditions (e.g., water temperature, salinity, and prey density), and the growth rates and spatial distributions of chum salmon. Perry et al. (1996) used the bioenergetics model developed by Ware (1978), which was developed as a general relationship for pelagic fish, and parameterized for sockeye salmon, to estimate the growth of the juvenile pink and chum salmon during migrations along the coast of Vancouver Island, British Columbia, Canada. Orsi et al. (2004) used the Wisconsin Bioenergetics Model 3.0 (Hanson et al., 1997) to estimate zooplankton prey consumption of juvenile chum salmon in southeastern Alaska. Kamezawa et al. (2007) and Kishi et al. (2010) developed a bioenergetics model for chum salmon to investigate the reduction in body size of Japanese chum salmon from the 1970s to 1990s. Their bioenergetics model was based on earlier fish bioenergetics models (Ware, 1978; Rudstam, 1988; Beauchamp et al., 1989; Trudel et al., 2004), and coupled with a three dimensional ecosystem model (Aita et al., 2007). Kishi et al. (2010) also reported the impact of global warming on chum salmon, including the migration of chum salmon northward to the Arctic Ocean during summer and significant decreases in the carrying capacity in subarctic areas.

Previous studies of chum salmon have mainly been undertaken in the North Pacific, which is a major rearing area, and have considered the habitat responses of global warming through only surface thermal limits (i.e., SST), despite the importance of prey density and the vertical migration of chum salmon. The extent of SST-based habitats can be underestimated for fishes migrating vertically, and can be overestimated by neglecting prey densities. Therefore, in this study, we estimated the potential habitat for chum salmon in the Western Arctic using a bioenergetics model coupled with the output data from a three-dimensional lower trophic ecosystem model, under both current conditions and a global warming scenario.

Chum salmon can be divided into Asian and North American groups, with juveniles recruited into the North Pacific north of 33°N on the Asian coasts, and north of 43°N on the North American coasts, respectively (Neave et al., 1976). Although chum salmon are divided into several groups by spawning ground, we did not consider the difference among the groups but considered all chum salmon migrating northward from the Bering Sea to the Western Arctic. This is because the available SST for all regional chum salmon ranged from 5 °C to 12 °C in the North Pacific including the Bering Sea during summer 1972–2002 (Nagasawa and Azumaya, 2009), and from 6.6 °C to 11.9 °C in the Bering Sea and the adjacent North Pacific during summer and fall 2002–2004 (Sato et al., 2009a), corresponding to the range of temperatures that may be adapted to for available habitats (5–13 °C) reported by Kaeriyama et al. (2012).

Model description

In this study, we used the chum salmon bioenergetics model developed by Kamezawa et al. (2007) and Kishi et al. (2010) (see detail in Section 'Bioenergetics model' and the Appendix A), and applied three-dimensional lower trophic ecosystem model results of Watanabe et al. (2012) as a simulated prey field for chum salmon. Watanabe et al. (2012) used the coupled sea ice–ocean model, which is composed of a physical ocean general circulation model called the Center for Climate System Research Ocean Component Model (COCO) (Hasumi, 2006), and a lower trophic marine ecosystem component, called the North Pacific Ecosystem Model for Understanding Regional Oceanography (NEMURO) (Kishi et al., 2007). The model domain covers the entire Chukchi Sea and the southern area of the Canada Basin (Fig. 2). The horizontal resolution is approximately 2.5 km, and there are 25 vertical levels (surface to 4000 m). The three-dimensional (3-D) NEMURO model (i.e., the coupled COCO and NEMURO model) was run for 9 months (from March to November 2003), without preceding spin-up run to avoid unexpected influence of the lateral boundary conditions, covering the entire period when chum salmon are present in the Bering Sea (i.e., June to November) (Urawa, 2000; Azumaya and Ishida, 2004). Furthermore, to evaluate the extent of potential chum salmon habitat under global warming, the model was run

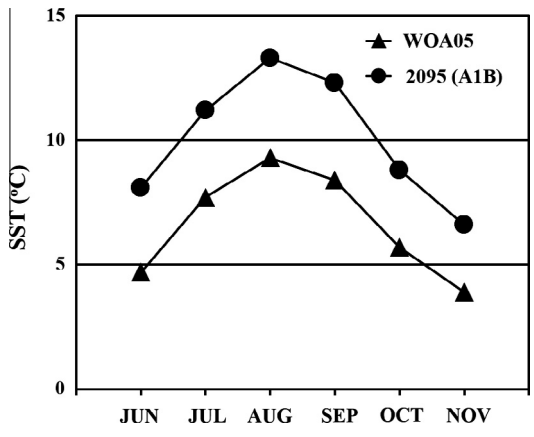

Fig. 1. Sea surface temperature (SST) in the Bering Sea (averaged over the region in 163.5°E to 200.5°E and 55.5°N to 65.5°N). Triangles indicate the current SST obtained from World Ocean Atlas 2005 (WOA05) and circles indicate the projected SST in 2095 (averaged from 2091 to 2100) simulated under a global warming scenario (SRES A1B) by Kawamiya et al. (2005) (2095 (A1B)).

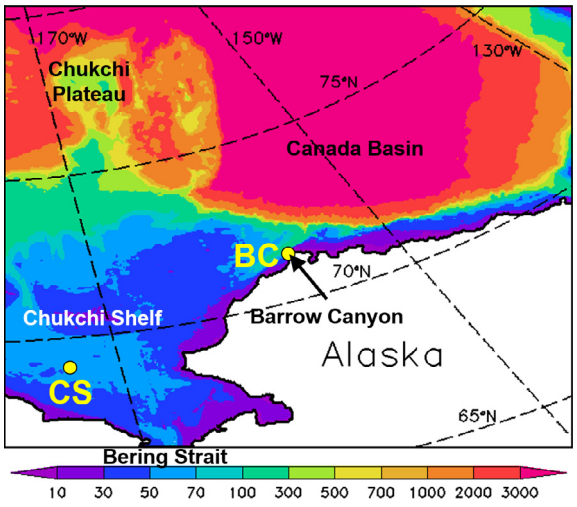

Fig. 2. Model bathymetry, together with two model output points (yellow circles of CS (173°W 69°N) and BC (157°W 71.4°N) referred to in Figs. 9 and 12). Shading indicates bathymetry (m).

under the IPCC SRES A1B (see detail in Section 'Global warming scenario').

Bioenergetics model

The bioenergetics model was based on the model for Atlantic herring proposed by Rudstam (1988). The growth rate of an individual chum salmon was represented by the wet weight increment per day:

$$\frac{dW}{dt} = [C - (R + SDA + F + E)] \cdot \frac{CAL_z}{CAL_f} \cdot W \quad (1)$$

where W is the wet weight of the fish (g wet weight; g WW or g fish), C is the consumption (g prey g fish^{-1} d^{-1}), R is the respiration or losses through metabolism (g prey g fish^{-1} d^{-1}), SDA is the specific dynamic action or losses due to the energy costs of digesting food (g prey g fish^{-1} d^{-1}), F is the egestion or losses in feces (g prey g fish^{-1} d^{-1}), E is the excretion or losses of nitrogenous excretory wastes (g prey g fish^{-1} d^{-1}), and CAL_z and CAL_f are the caloric equivalent of prey (i.e., zooplankton) (cal g prey^{-1}) and fish (cal g fish^{-1}), respectively:

$$CAL_z = \frac{2580\ J}{1\ g\ prey} \times \frac{1\ cal}{4.18\ J} = 617.22\ cal\ g\ prey^{-1} \quad (2)$$

$$CAL_f = \frac{5533\ J}{1\ g\ prey} \times \frac{1\ cal}{4.18\ J} = 1323.68\ cal\ g\ fish^{-1} \quad (3)$$

The formulations for the individual processes were the same as those reported in Kamezawa et al. (2007) and Kishi et al. (2010) and are listed in the Appendix A; parameter values are given in Table 1. The life stages of Japanese chum salmon were divided into eight stages according to the age-specific habitat distribution based on Urawa (2000): stage 1 (1–1.5 years old; the number of years after fertilization) was in the Western North Pacific, stages 2 (1.5–2.0 years old), 4 (2.5–3.0 years old), 6 (3.5–4.0 years old), and 8 (4.5–5.0 years old) were in the Bering Sea, and stages 3 (2.0–2.5 years old), 5 (3.0–3.5 years old), and 7 (4.0–4.5 years old) were in the Eastern North Pacific (Fig. 3). According to their results (i.e., Kamezawa et al. (2007) and Kishi et al. (2010)), the stage-specific body weight of chum salmon was about 500 g WW in stage 2, 1000–1500 g WW in stage 4, 1500–3000 g WW in stage 6, and 2000–3500 g WW in stage 8. In this study, we focused upon chum salmon migrating northward from the Bering Sea to the Western Arctic, thus we used the parameter values for stages 2, 4, 6, and 8, in which chum salmon were in the Bering Sea between June and November. Using the bioenergetics model, the growth rates of 100–4000 g WW chum salmon were calculated for the entire model domain shown in Fig. 2, and vertically from the surface to 100 m, because chum salmon migrate vertically to below 100 m to control their body temperature and search for prey (Walker et al., 2000; Ishida et al., 2001; Azumaya and Ishida, 2005).

Inputs from the 3-D NEMURO model

The water temperature, salinity, and prey density values in the bioenergetics model were obtained from the 3-D NEMURO model results simulated by Watanabe et al. (2012). The NEMURO model has three categories of zooplankton: (1) small zooplankton (ZS), (2) large zooplankton (ZL), and (3) predatory zooplankton (ZP) (Kishi et al., 2007). Kamezawa et al. (2007) and Kishi et al. (2010) assumed that modeled chum salmon prey upon ZP because chum salmon select their diets from gelatinous zooplankton and more nutritious species (Tadokoro et al., 1996; Kaeriyama et al., 2004), thus we followed the same assumption. ZP, as a top predator in the NEMURO model, includes all carnivorous zooplankton (i.e., gelatinous zooplankton, euphausiids, and other large carnivorous zooplankton), and these are not further resolved in the model. The available prey field for chum salmon might be overestimated by including non-prey species in ZP, although it has been reported that chum salmon could shift their diets based on prey availability and/or interspecific competition (Tadokoro et al., 1996; Kaeriyama et al., 2004; Cook and Sturdevant, 2013) (see more in Section 'Conclusions'). The NEMURO describes zooplankton density as nitrogen density (μmol N L^{-1}), and we converted it into wet weight following Megrey et al. (2002):

$$\frac{14\ \mu\ gN}{1\ \mu\ mol\ N} \times \frac{10^{-6}\ g}{1\ \mu\ g} \times \frac{1\ g\ dry\ weight}{0.07\ g\ N} \times \frac{1\ g\ wet\ weight}{0.2\ g\ dry\ weight} \times \frac{10^3\ L}{1\ m^3} \quad (4)$$

The modeled SST, chlorophyll *a*, and nitrate were found to show good agreement with Moderate-Resolution Imaging Spectroradiometer and World Ocean Atlas 2009 data (Watanabe, 2011; Watanabe et al., 2012). However, the model validation of zooplankton biomass remains to be completed, although the modeled ZL biomass was compared with the copepod biomass obtained from Campbell et al. (2009) (Watanabe et al., 2012). In Section 'Comparisons between observations and model results for zooplankton biomass', we compare the zooplankton biomass with previous observations (Sherr et al., 2009; Campbell et al., 2009; Hopcroft et al., 2010) and the model results by Watanabe et al. (2012).

Table 1
Parameter values used in the chum salmon bioenergetics model (Kamezawa et al., 2007; Kishi et al., 2010).

Symbol	Parameter description	Value
Consumption, C_{MAX}		
ac	Intercept for C_{MAX} parameter	0.303
bc	Coefficient for C_{MAX} parameter versus weight	-0.275
V_i	Vulnerability constant	1.0
K_i	Half saturation constant	0.15
xk1	Proportion of C_{MAX} for te1	0.30
xk2	Proportion of C_{MAX} for te2	0.98
xk3	Proportion of C_{MAX} for te3	0.98
xk4	Proportion of C_{MAX} for te4	0.5
te1	Temperature for xk1	3.0
te2	Temperature for xk2	5.0
te3	Temperature for xk3	10.0
te4	Temperature for xk4	12.0
Metabolism, R		
ars	Intercept for standard metabolic rate of 1 g fish at 0 °C	0.0799
br	Coefficient for standard metabolism versus body weight	0.8
cr	Coefficient for standard metabolism versus temperature	0.069
ara	Intercept for swimming cost	Eq. (A.16)
dr	Coefficient for swimming cost versus body weight	0.44
er	Coefficient for swimming cost versus temperature	2.42
Swimming speed, U		
au	Intercept for optimal foraging speed	20.3
bu	Coefficient for swimming speed versus weight	0.132
Specific dynamic action, SDA		
ss	Coefficient for specific dynamic action	0.175
Egestion, F and Excretion, E		
af	Proportion of consumed food egested	0.16
ae	Proportion of consumed food excreted	0.1
Caloric value		
CAL_z	Caloric equivalent of zooplankton	617.22
CAL_f	Caloric equivalent of fish	1323.68

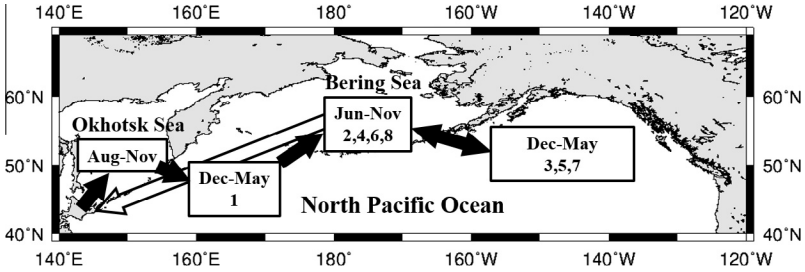

Fig. 3. Schematic view of the migration route of Japanese chum salmon (modified from Urawa 2000). The months in boxes indicate the period when chum salmon are distributed in each sea. The numbers in boxes indicate life stages of chum salmon according to the age-specific habitat distribution: stage 1 (1–1.5 years old; the number of years after fertilization) is in the Western North Pacific, stages 2 (1.5–2.0 years old), 4 (2.5–3.0 years old), 6 (3.5–4.0 years old), and 8 (4.5–5.0 years old) is in the Bering Sea, and stages 3 (2.0–2.5 years old), 5 (3.0–3.5 years old), and 7 (4.0–4.5 years old) is in the Eastern North Pacific (Kamezawa et al. 2007; Kishi et al. 2010).

Definition of potential habitat

We defined "potential habitat" as "an area where chum salmon could grow (i.e., dW/dt > 0 in Eq. (1))". This definition was based on the hypothesis that chum salmon would migrate for survival, feeding, and growth to maturity except during their homing migration (this study targeted on feeding migration only). In the bioenergetics model reported in Kamezawa et al. (2007) and Kishi et al. (2010), the weight-specific range of prey density (i.e., ZP biomass) and water temperature for the positive growth potential of 100–4000 g WW chum salmon at a salinity of 33.0 is shown in Fig. 4. The contours indicate the conditions for the positive growth rate of chum salmon of 500, 1000, 1500, 2000, 2500, 3000, and 3500 g wet weight, and the regions bounded by the contours indicate the conditions for their "potential habitat" as: from violet to orange, shading indicates the habitat for chum salmon below 500, 1000, 1500, 2000, 2500, 3000, and 3500 g WW, and the red-shaded area indicates the habitats for all chum salmon of 100–4000 g WW. The temperature range where growth is possible increases as the available prey density increases. The temperature range where growth is possible for 500 g WW chum salmon ranges from 3.3 °C to 12.1 °C under a prey density condition of 0.5 μmol N L^{-1}, and its range decreases as the body weight increases; 3.4 °C to 11.9 °C for 1000 g WW, 3.7 °C to 11.6 °C for 2000 g WW, and 3.8 °C to 11.4 °C for 3000 g WW chum salmon. The minimum prey densities where growth is possible are 0.08, 0.11, 0.16, and 0.21 μmol N L^{-1} for 500, 1000, 2000, and 3000 g WW chum salmon, respectively. The growth rate decreases as the salinity increases due to the increased metabolism of the fish (Eq. (A.16)).

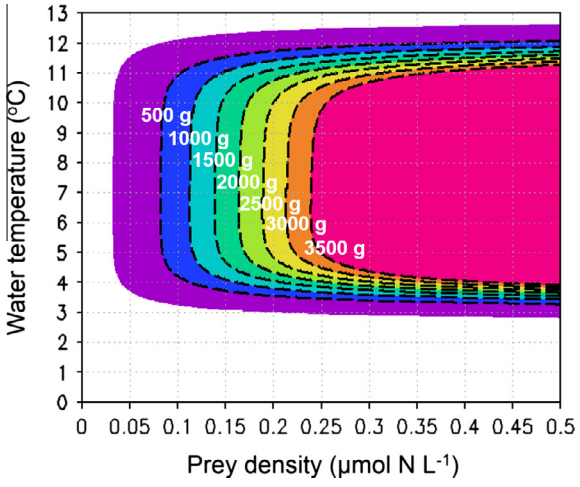

Fig. 4. Weight-specific prey densities (i.e., predatory zooplankton biomass, ZP) and water temperatures required for positive growth potential (i.e., dW/dt > 0) of chum salmon at a salinity condition of 33.0. The contours (dashed lines) indicate the conditions for the positive growth rate of chum salmon of 500, 1000, 1500, 2000, 2500, 3000, and 3500 g wet weight, and the regions bounded by the contours indicate the conditions for their "potential habitat" as: from violet to orange, shading indicates the habitat for chum salmon below 500, 1000, 1500, 2000, 2500, 3000, and 3500 g WW, and the red-shaded area indicates the habitats for all chum salmon of 100–4000 g WW. (For interpretation of the references to colour in this figure legend, the reader is referred to the web version of this article.)

Global warming scenario

To evaluate the habitat extent under global warming conditions, we used the monthly changes in water temperature simulated under the IPCC SRES A1B (Kawamiya et al., 2005), using the Model for Interdisciplinary Research on Climate (Hasumi and Emori, 2004). The monthly changes were calculated by subtracting the simulated monthly temperature data in 2005 (averaged from 2001 to 2010) from those in 2095 (averaged from 2091 to 2100). The changes were interpolated spatially to the COCO model grids and temporally to the model time step, and they were then added to the water temperature for calculation of biogeochemical processes in the 2003 case simulated by Watanabe et al. (2012). Using this water temperature, the 3-D NEMURO was run again to obtain the ZP biomass (i.e., prey density) under the global warming scenario. We changed only water temperature used for NEMURO calculations in the global warming scenario: all other physical conditions, such as atmospheric forcing, river runoff, sea ice, salinity, and circulation patterns were identical between the current and global warming scenario experiments. The monthly changes in water temperature and normalized ZP biomass between the current and global warming scenario are shown in Fig. 5(a) and (b), and monthly water temperatures in 2003 and 2095 used in this study are shown in Fig. 5(c) and (d). The values are expressed as values averaged horizontally over the entire model domain as shown in Fig. 2. The normalized change in ZP biomass was calculated as: (ZP in 2095)/(ZP in 2003) – 1, where (ZP in 2003) is the ZP biomass in the 2003 case simulated by Watanabe et al. (2012) and (ZP in 2095) is the ZP biomass in 2095 (averaged from 2091 to 2100) simulated in this study using the 3-D NEMURO. The change in water temperature increases from June to July and decreases from July to November with a minimum at a depth of 50–70 m (Fig. 5(a)). The change in ZP increases from June to August for the surface to 40 m, to September for 40–60 m, to October for 60–80 m, and to November below 80 m (Fig. 5(b)).

Results and discussion

Comparisons between observations and model results for zooplankton biomass

The zooplankton biomass in the Western Arctic has been studied previously. Sherr et al. (2009) and Campbell et al. (2009) inves-

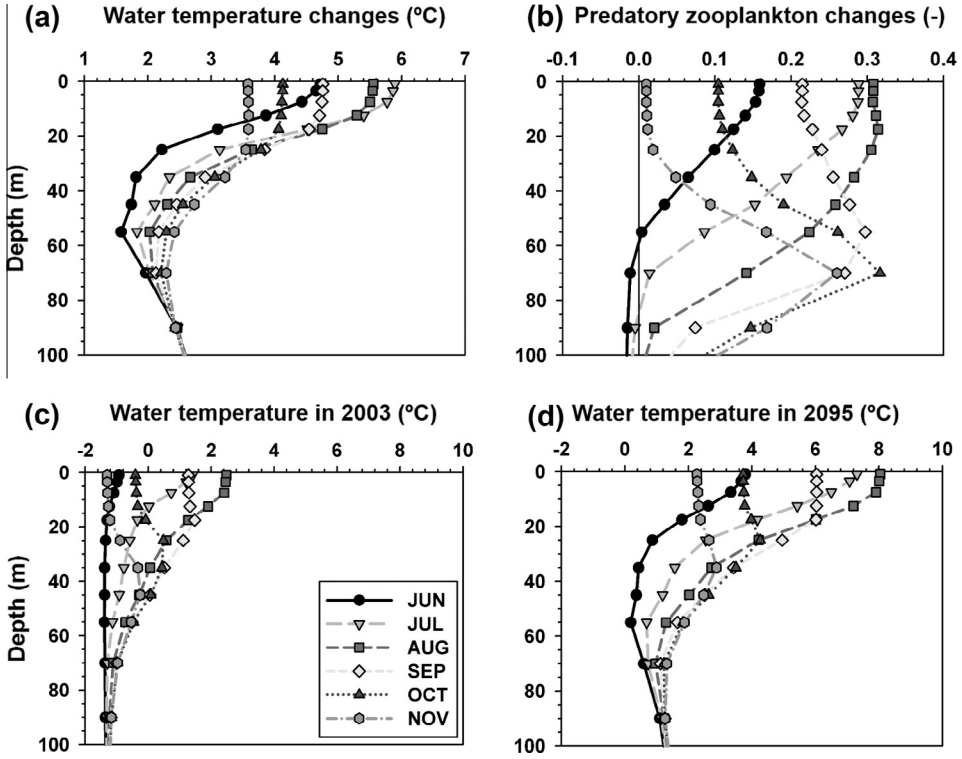

Fig. 5. (a) Monthly change in water temperatures between 2005 (averaged from 2001 to 2010) and 2095 (averaged from 2091 to 2100) simulated under the SRES A1B by Kawamiya et al. (2005), and (b) normalized change between the predatory zooplankton (ZP) biomass in the 2003 case simulated by Watanabe et al. (2012) and the ZP biomass in 2095 simulated in this study under the global warming scenario SRES A1B, and water temperatures in (c) 2003 and (d) 2095 used in this study. The values are expressed as values averaged horizontally in the entire model domain as shown in Fig. 2.

tigated the zooplankton community in the upper 100 m of the Chukchi and Beaufort shelf, slope, and basin regions during summer (the end of July to the middle of August) 2002 and 2004. Sherr et al. (2009) estimated that the total ciliate biomass (corresponding to ZS in the 3-D NEMURO) ranged to 0.5–25 μg C L^{-1}, and Campbell et al. (2009) estimated that the total copepod biomass (corresponding to ZL) ranged from 2 to 5 g C m^{-2}. Hopcroft et al. (2010) conducted zooplankton sampling in the Chukchi Sea in August 2004, and estimated that the total biomass of holozooplankton was 42 mg dry weight m^{-3} (mg DW m^{-3}), in which the total copepod biomass was 30 mg DW m^{-3}. Fig. 6 shows the model-estimated mean August biomasses of ZS, ZL, and ZP under current conditions. The model results are expressed as values are averaged vertically over the upper 100 m to correspond to ocean observations conducted from the surface to a depth of 100 m. The rectangle and ellipse in each figure indicate the locations observed in previous studies (i.e., Sherr et al. (2009) and Campbell et al. (2009) in the rectangle, and Hopcroft et al. (2010) in the ellipse). For the comparison between these observations and model results, the unit of model results (μmol N L^{-1}) was converted into units of observational data (mg DW m^{-3}, or μg C L^{-1}, or g C m^{-2}) based on Eq. (4) and a Redfield ratio (C:N) of 106:16. In the rectangular areas shown in Fig. 6, ZS ranges from 0.01 to 0.06 μmol N L^{-1} (1–5 μg C L^{-1}), which corresponds to the range of 0.5–25 μg C L^{-1} reported by Sherr et al. (2009), and ZL ranges from 0.1 to 0.7 μmol N L^{-1} (0.8–5.6 g C m^{-2}), which corresponds to the range of 2–5 g C m^{-2} reported by Campbell et al. (2009). In the area of the ellipse in Fig. 6, ZL ranges from 0.5 to 1.2 μmol N L^{-1} (100–240 mg DW m^{-3}), which is higher than the 30 mg DW m^{-3} reported by Hopcroft et al. (2010). In the same area, ZP is

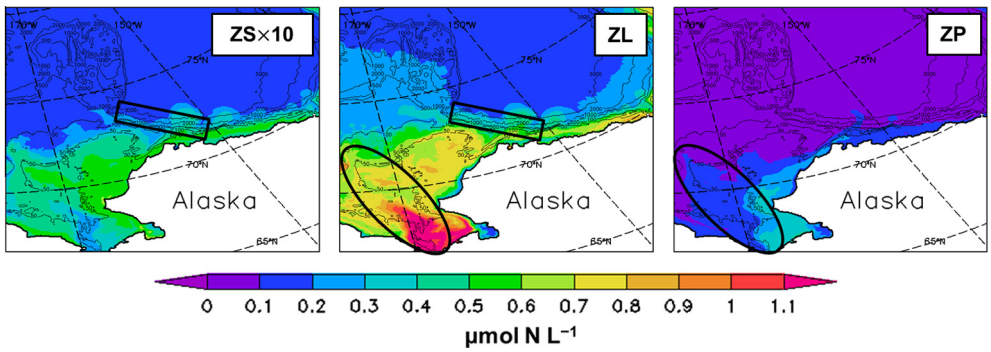

Fig. 6. Mean August small zooplankton (ZS), large zooplankton (ZL), and predatory zooplankton (ZP) biomasses (μmol N L^{-1}) averaged vertically in the upper 100 m of the Western Arctic under current conditions as simulated by Watanabe et al. (2012). ZS biomass is multiplied by 10. The rectangle and ellipse in each figure indicate the locations observed in previous studies (i.e., Sherr et al. (2009) and Campbell et al. (2009) in the rectangle and Hopcroft et al. (2010) in the ellipse).

~0.4 μmol N L^{-1} (~80 mg DW m^{-3}). If we assume that all zooplankton, except for copepods in Hopcroft et al. (2010) are ZP, the ZP/ZL ratio would be 0.4 (12 mg DW m^{-3}/30 mg DW m^{-3}), which corresponds to the model result of 0.25–0.5. The above results are summarized in Table 2. The model results in the northern part of the Chukchi Sea show good agreement with previous observations. The model results in the southwestern part are within the same order of magnitude as the observations, although the model results slightly overestimate observed values. Therefore, we considered it to be appropriate to use the 3-D NEMURO model results simulated by Watanabe et al. (2012) as input data for the bioenergetics model of chum salmon to estimate their potential habitat in the Western Arctic.

Potential habitat for chum salmon under current conditions

The estimated monthly weight-specific potential habitat is shown in Fig. 7. The potential habitat of larger chum salmon includes the habitat for smaller salmon. The potential habitat is restricted to the southwestern Alaskan coast in June, and expands to the Chukchi Shelf and along the northwestern Alaskan coast from July to September, and contracts in October. The potential habitat reflects the warm and nutrient-rich Pacific water inflowing from the Bering Strait. The northward Bering Strait through flow is diverted into three branches following major features of the bottom topography over the broad and shallow Chukchi Shelf. One branch flows northwest, and the other two branches flow northeast through the central channel of the Chukchi Shelf and along the Alaskan coastline, respectively. The Pacific water transport reaches a maximum during late summer and early autumn and is at a minimum in mid-winter (Watanabe and Hasumi, 2009; Watanabe, 2011).

Fig. 8(a) shows the monthly mean maximum-growth depth (MGD) for 500 g WW chum salmon in September, when the potential habitat area is the largest. The MGD changes due to environmental conditions (i.e., water temperature and prey density), and the body weight of chum salmon. In the southern part of the model domain, the MGD is located near the surface where both water temperature and prey density are higher. The MGD deepens with increasing latitude (i.e., a decrease in water temperature and prey density), because energy loss decreases in colder water (i.e., deeper

Table 2
Summary of observations and model results for zooplankton biomass in the regional areas shown in Fig. 6.

Symbol	Source	Observation	Model result[f]	
ZS[a]	Sherr et al. (2009)	0.5–25 μg C L^{-1}	1–5 μg C L^{-1}	0.01–0.06[g]
ZL[b]	Campbell et al. (2009)	2–5 g C m^{-2}	0.8–5.6 g C m^{-2}	0.1–0.7[g]
ZL[c]	Hopcroft et al. (2010)	30 mg DW m^{-3}	100–240 mg DW m^{-3}	0.5–1.2[g]
ZP[d]		12 mg DW m^{-3}	~80 mg DW m^{-3}	~0.4[g]
ZP/ZL[e]		0.4	0.25–0.5	

[a] Small zooplankton (ZS) in the rectangular area shown in Fig. 6.
[b] Large zooplankton (ZL) in the rectangular area shown in Fig. 6.
[c] Large zooplankton (ZL) in the ellipse shown in Fig. 6.
[d] Predatory zooplankton (ZP) in the ellipse shown in Fig. 6.
[e] The ratio between ZP and ZL in the ellipse shown in Fig. 6.
[f] The unit of model results (μmol N L^{-1}) is converted into the unit of observational data (mg DW m^{-3}, or μg C L^{-1}, or g C m^{-2}) based on Eq. (4) and a Redfield ratio (C:N) of 106:16.
[g] μmol N L^{-1}.

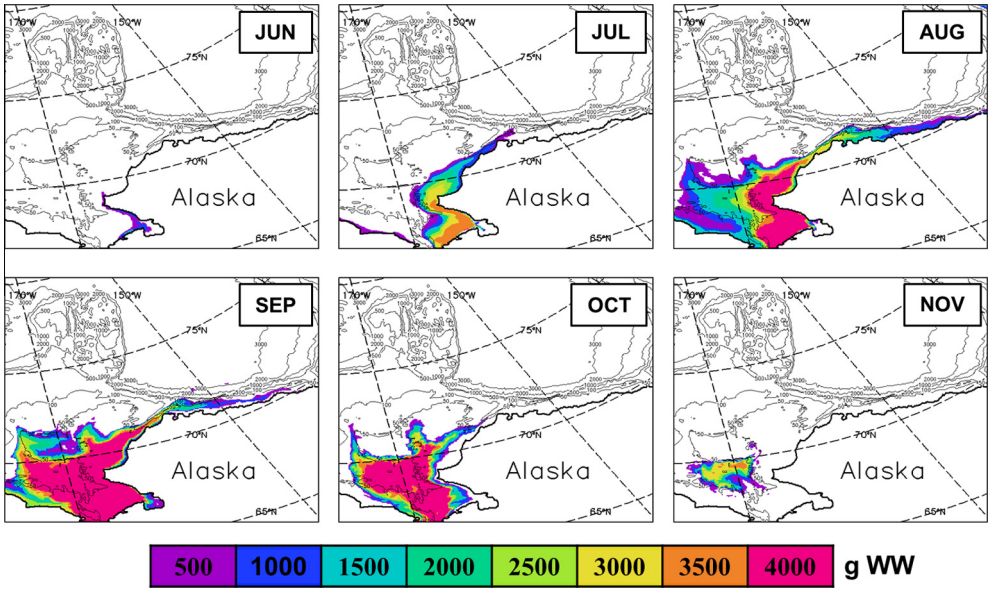

Fig. 7. Estimated weight-specific potential habitat for chum salmon at the maximum-growth depth in the Western Arctic from June to November under current climate conditions. The potential habitat of larger chum salmon includes the habitats for smaller salmon: violet-shaded areas indicate the habitats for 100–500 g WW chum salmon and red-shaded areas indicate the habitats for all chum salmon of 100–4000 g WW. (For interpretation of the references to colour in this figure legend, the reader is referred to the web version of this article.)

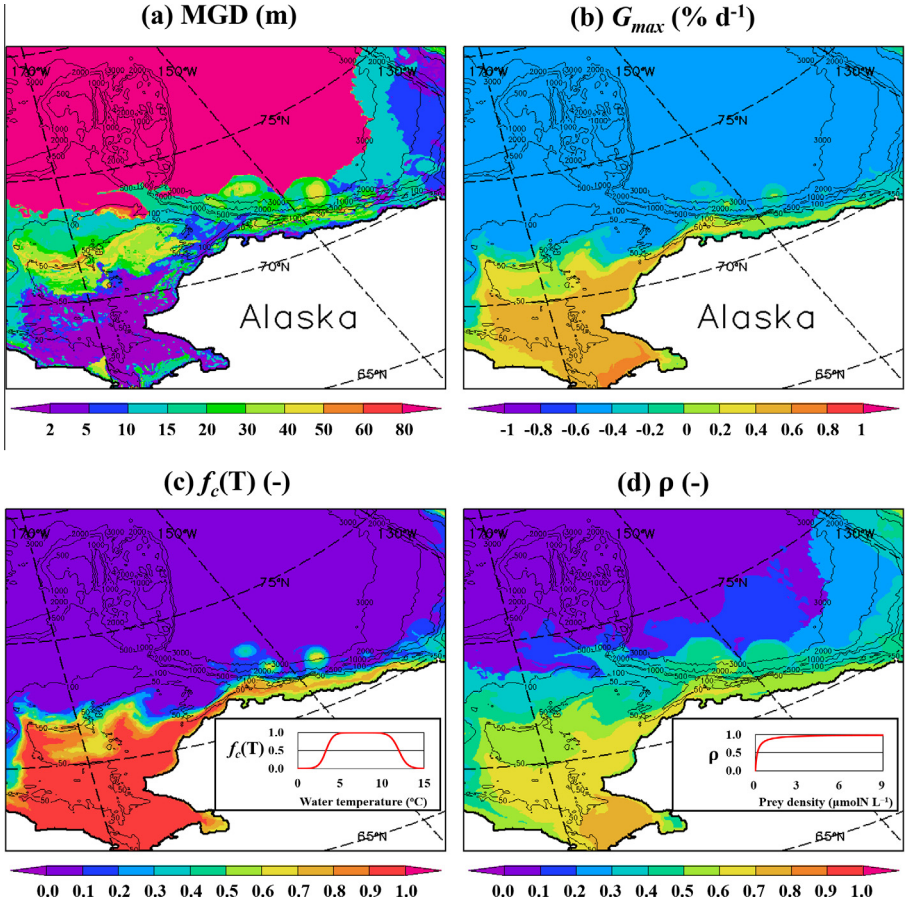

Fig. 8. September mean (a) maximum-growth depth (MGD; m) of 500 g WW chum salmon, (b) the maximum growth rate (G_{max}; % d^{-1}), and (c) the temperature dependence function for consumption (f_c(T) in Eq. (A.4); dimensionless) and (d) the available consumption rate without temperature effects (ρ in Eq. (A.3); dimensionless) at the MGD under current climate conditions. The inset graphs in (c) and (d) show the ranges of f_c(T) and ρ.

layers) (Eqs. (A.13)–(A.16)). The MGD is located at a depth of 80–100 m in most of the northern part of model domain. Fig. 8 (b) shows the September mean growth rate of 500 g WW chum salmon at the MGD (i.e., the maximum growth rate; G_{max}). Fig. 8 (c) and (d) show the temperature dependence function for consumption ($f_c(T)$ in Eq. (A.4)) and the available consumption rate without temperature effects (ρ in Eq. (A.3)), respectively. Both an $f_c(T)$ and ρ of 1.0 indicate that consumption is not limited by water temperature and prey density. An $f_c(T)$ of 0.8 and ρ of 0.5 indicate that the consumption is 80% limited by the water temperature and 50% limited by the prey density, thus consumption is only 40% of the maximum (i.e., the $f_c(T) \times \rho = 0.4$). Both the $f_c(T)$ and ρ decrease with increasing latitude (i.e., a decrease in water temperature and prey density), and are almost zero in the northern part of the domain. Furthermore, north of Barrow Canyon in Fig. 8, the MGD is shallower and G_{max}, $f_c(T)$, and ρ are higher in a couple of eddies than the surrounding basin area, because the shelf-break eddies transport heat and nutrients originating in the shelf with high primary productivity toward the Canada Basin (Watanabe et al., 2012; Watanabe et al., 2014).

Fig. 9 shows seasonal transitions in the vertical potential habitat, the MGD, the G_{max}, and the $f_c(T)$ and ρ at the MGD, at two representative points (i.e., CS and BC) in Fig. 2. CS is a point on the northwest branch of the Bering Strait through flow on the Chukchi Shelf, and was the location where the potential habitat persisted through to November (Fig. 7). BC is a coastal point in the Barrow Canyon which is an important passage for the transport of Pacific water from the Chukchi Shelf to the Canada Basin (Watanabe et al., 2012; Watanabe et al., 2014). At CS, a potential habitat forms at the surface at the end of July, and disappears at the surface in November, and the duration that the habitat remains suitable shortens as the body weight increases (Fig. 9(a)). The MGD gradually deepens as the upper layer cools from October. At BC, the potential habitat forms at all depths at about the same time in the middle of July, which is half a month earlier than at CS, and then disappears in the beginning of October (Fig. 9(b)). The MGD rapidly deepens with cooling in the surface and middle layers in October, and the MGD is near the surface where prey density is higher (but this is not as significant; data not shown) in November when cold water reaches the bottom. The f_c(T) is close to zero in the beginning of June, and increases by almost 1.0 at both CS and BC at the end of June due to the rapid warming associated with the retreat of sea ice and the Pacific water inflow (Fig. 9(c) and (d)). The high $f_c(T)$ continues to November at CS and August at BC, and then rapidly decreases in October at BC. The ρ begins to increase from June due to the increase in prey density with increasing water temperature, but the prey density is not sufficient for the growth of chum salmon by the beginning of July. This explains why CS and BC do not constitute a potential habitat, although the f_c(T) is almost 1.0 at the end of June to the beginning of July. When the ρ is above about 0.35, a potential habitat for 500 g WW chum salmon forms. The ρ reaches a maximum of about 0.7 in October at CS and 0.65 in September at BC.

Our results are supported by previous studies. Echave et al. (2012) identified the essential fish habitat (EFH) for five species of Pacific salmon, including chum salmon in the US Exclusive Eco-

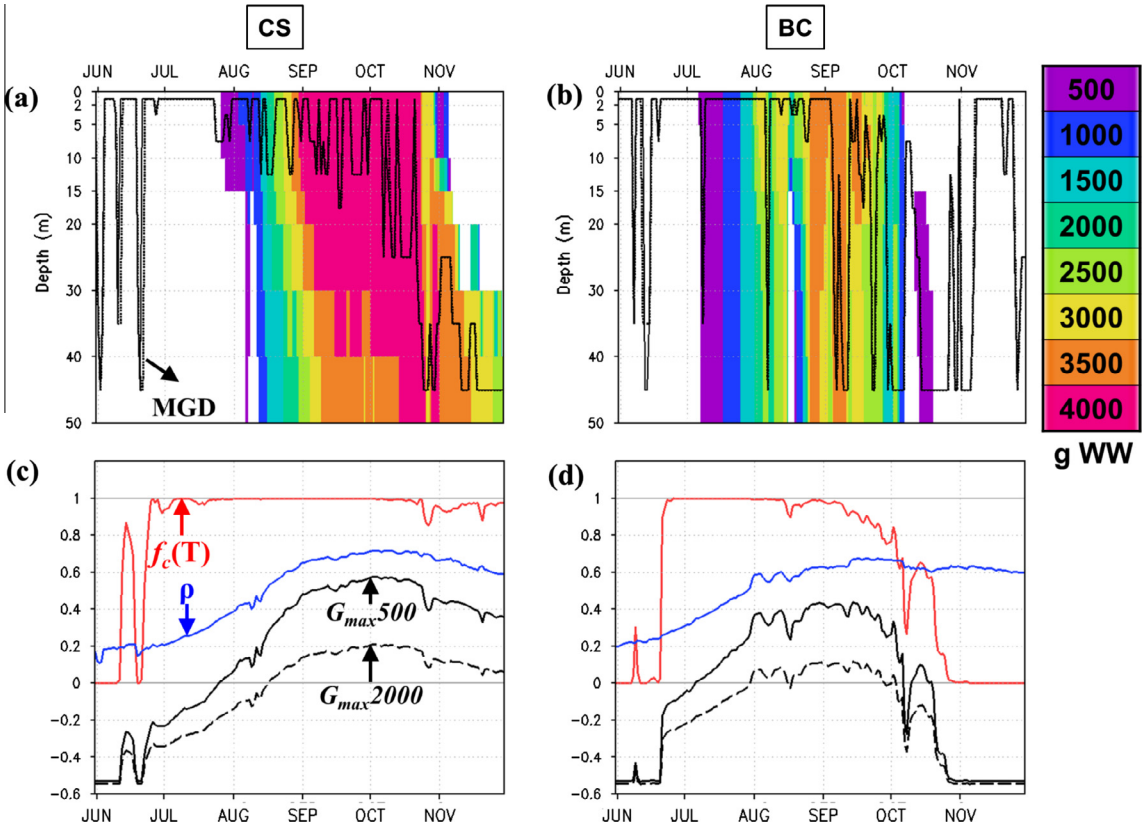

Fig. 9. Seasonal transitions in the vertical potential habitat (color-shaded areas), the maximum-growth depth (MGD; m) of 500 g WW (black solid line in (a) and (b)) and 2000 g WW chum salmon (dotted line), the maximum growth rates of 500 g WW (G_{max}500; % d^{-1}; black solid line in (c) and (d)) and 2000 g WW chum salmon (G_{max}2000; % d^{-1}; black dashed line), and the temperature dependence function for consumption ($f_c(T)$; dimensionless; red line) and the available consumption rate without temperature effects (ρ; dimensionless; blue line) at the MGD at two model output points (CS and BC in Fig. 2) from June to November under current conditions. Shading is same as in Fig. 7. The model results are expressed as daily mean values. (For interpretation of the references to colour in this figure legend, the reader is referred to the web version of this article.)

nomic Zone using catch, maturity, salinity, temperature, and depth obtained from multiple data sources (e.g., Bering-Aleutian Salmon International Survey transect data, Southeast Alaska Coastal Monitoring data, Canadian Fisheries and Oceans salmon data, Coastal Gulf of Alaska data, and many other coastal salmon survey data). Their EFH for chum salmon also includes the Chukchi Sea. Sato et al. (2012) surveyed the chum salmon distribution from the Bering Sea to the Chukchi Sea during the periods of 15–24 July and 30 July to 9 August, 2009. From their results, the mean catch per unit effort (CPUE) was about 165.7 in the Bering Sea (52°N to 58°N), 301.0 in the Northern Bering Sea (59°N to 63°N), 4.2 in the Bering Strait (64°N to 65°N), and 3.7 in the Chukchi Sea (67°N to 70°N). Morita et al. (2009), which is the same observation as Sato et al. (2012), also reported that four large chum salmon (more than 2000 g) were caught in the Chukchi Sea (68°N to 70°N) (CPUE = 1.3), which corresponds to the potential habitat in July and August. The CPUE was lower in the Chukchi Sea than in the Bering Sea, however, which is important evidence that chum salmon can migrate from the Bering Sea to the Chukchi Sea during summer. Morita et al. (2009) and Nagasawa and Azumaya (2009) reported that the trend in distribution appeared to be for larger chum salmon to be found further to the north in the Bering Sea and the North Pacific. Larger chum salmon must have been distributed further to the cooler north due to the increase in water temperature because the maximum water temperature for positive growth rate of larger chum salmon is lower than that of smaller chum salmon (Fig. 4). On the other hand, modeled potential habitats for larger chum salmon are restricted to more southerly regions in the Western Arctic (Fig. 7) because the minimum water temperature for positive growth of larger chum salmon is higher than that of smaller chum salmon (Fig. 4).

Potential habitat under the global warming scenario

Under the global warming scenario, the potential habitat expands to the north compared with that under the current conditions, due to the increase in water temperature and prey density (Fig. 10). In contrast, south of 71°N during summer (July to September), the potential habitat shrinks regionally because the water temperature exceeds the optimal condition (5 °C to 10 °C in which the $f_c(T)$ is almost 1.0). South of 71°N, the potential habitat decreases in areas where the water depth is shallower than 30 m in July and August, but increases in areas where the water depth is deeper than 50 m. The reason for this is that the shallow area is easy to heat, even in the bottom layers, but the deep area retains optimal conditions in the middle or bottom layers despite the surface heating. In areas where the water depth is 30–50 m, the potential habitat increases for smaller chum salmon (~2000 g WW), but decreases for larger chum salmon (⩾2500 g WW) because the range of optimal conditions of larger chum salmon is narrower than that of smaller chum salmon. The changes in potential habitat due to global warming is mainly affected by the water depth in July and August, whereas those in September seem to affected by the longitude because oceanic conditions change with changing longitude. In September, the potential habitat increases west of 170°W with decreasing water temperature (i.e., the water

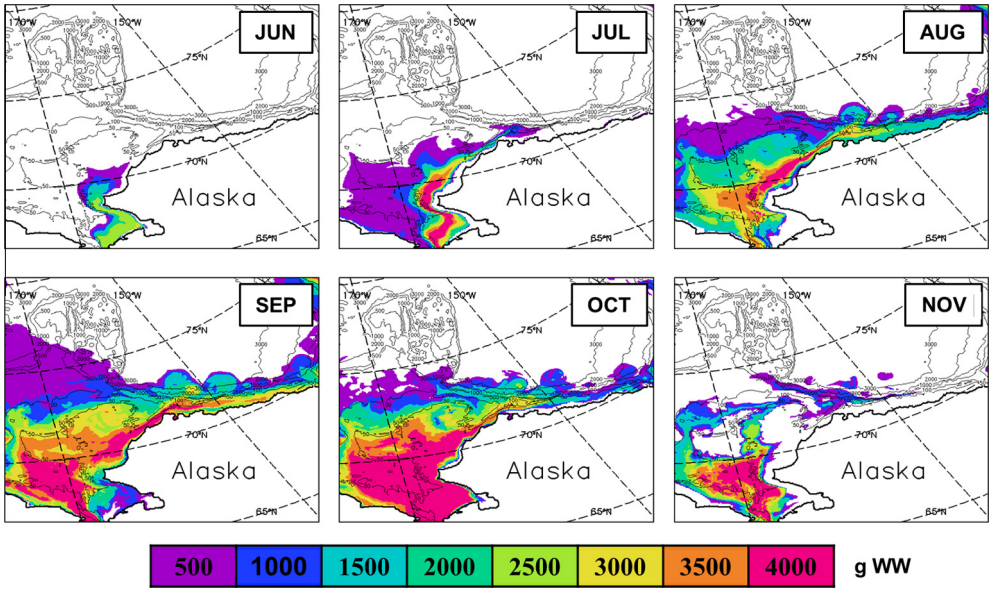

Fig. 10. Same as in Fig. 7 but for the global warming scenario (SRES A1B).

temperature does not exceed the optimal condition), and decreases east of 170°W where the water temperature is still high compared with that under the current conditions.

The MGD of 500 g WW chum salmon in September is deeper than under current conditions due to the high water temperature in the upper layer, in the southern parts of the model domain. There is an exception for locations near the coast, where the cooling is faster because of the shallow water depth, and the water temperature decreases to below optimum conditions at the surface (Fig. 11(a)). On the other hand, in the northern parts the MGD becomes shallower with increasing water temperature and prey density. The G_{max} increases, except for locations east of 170°W and south of 71°N where the water temperature still exceeds the optimal conditions under the global warming scenario

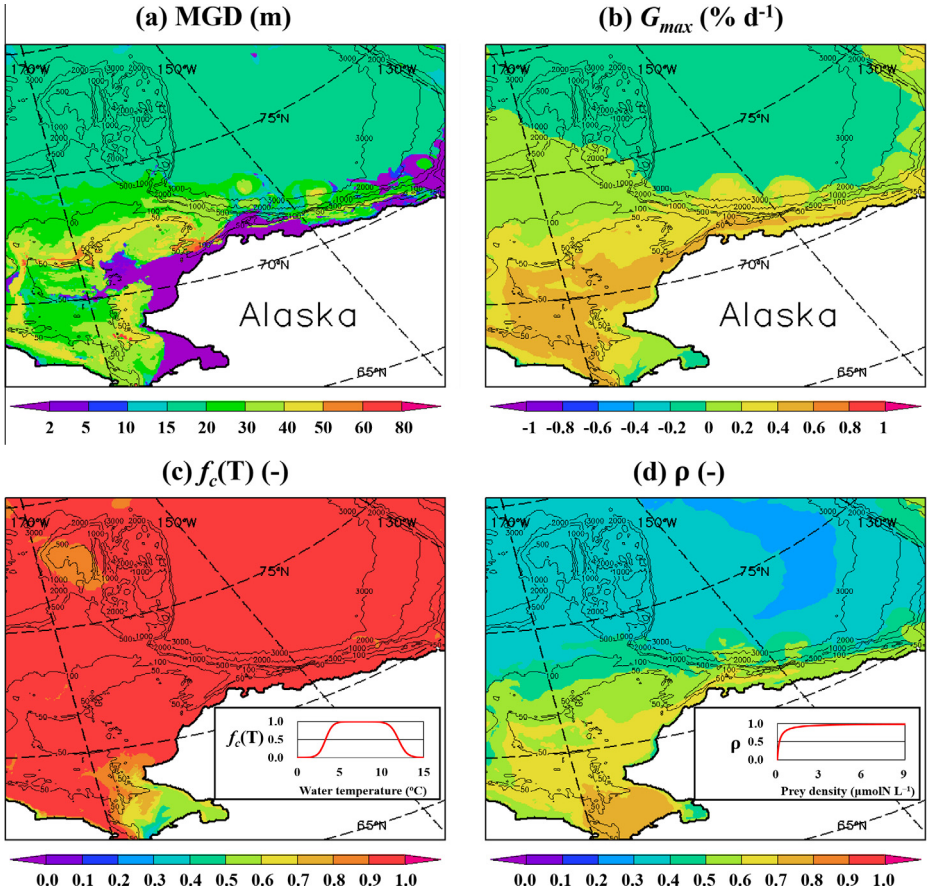

Fig. 11. Same as in Fig. 8 but for the global warming scenario (SRES A1B).

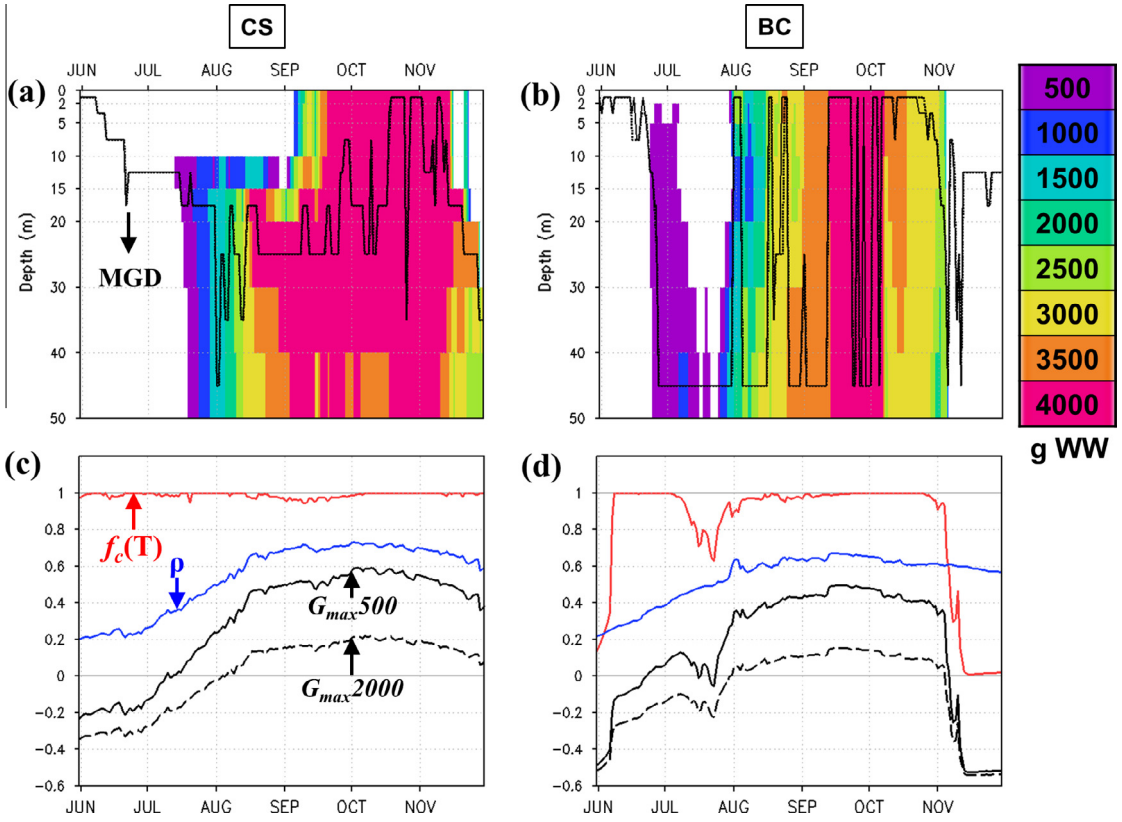

Fig. 12. Same as in Fig. 9 but for the global warming scenario (SRES A1B).

(Fig. 11(b)). The $f_c(T)$ increases to become close to 1.0, except for locations east of 170°W and south of 71°N (Fig. 11(c)). The ρ also increases, especially in the northern part of the domain, but not as significantly in the southern part (Fig. 11(d)).

At CS, the potential habitat forms from the middle of July and disappears at the surface in the middle of November (Fig. 12(a)). The MGD gradually deepens with surface heating from June, becomes shallower with cooling from September, and deepens again from the beginning of November because the water temperature decreases to below the optimal condition in the upper layer. The $f_c(T)$ is almost 1.0 throughout the model experiment period (Fig. 12(c)). The ρ is slightly higher than under current conditions and reaches 0.35 in the middle of July, which is about 10 days earlier than under current conditions (the significance of a value of 0.35 was discussed in Section 'Potential habitat for chum salmon under current conditions'). At BC, the potential habitat forms from the subsurface to the bottom at the end of June and disappears at the beginning of November (Fig. 12(b)). Changes in the MGD at BS are sharper than at CS because it is in the shallower area where changes in water temperature have more impact. The MGD rapidly deepens with surface heating at the end of June and becomes shallower with cooling in the middle of September. It deepens by 10–15 m where the water temperature is lightly warmer than at the surface. The f_c(T) rapidly increases by 1.0 at the beginning of June, but decreases during summer due to the water temperature exceeding the optimal conditions (Fig. 12(d)). The ρ reaches 0.35 10 days earlier, but is almost the same as that under the current conditions.

Conclusions

This study focused on chum salmon migrating northward from the Bering Sea to the Western Arctic and conducted a numerical modeling study to estimate the potential habitat for chum salmon in the Western Arctic. "Potential habitat" was defined as "an area where chum salmon could grow (i.e., the growth rate was positive)". The growth rate was calculated using a bioenergetics model coupled with a three-dimensional lower trophic ecosystem model, considering the prey density and vertical migration of chum salmon as well as the water temperature.

The potential habitat under current conditions was restricted to the southwestern Alaskan coast in June, but expanded to the Chukchi Shelf and along the northwestern Alaskan coast from July to September, and receded again in October. Under the global warming scenario, the potential habitat for chum salmon expanded to the north due to the increase in water temperature and prey density. In contrast, south of 71°N during summer, the potential habitat shrunk regionally because the water temperature exceeded the optimal condition. This indicated that the water temperature could also exceed the optimal conditions in the Bering Sea, and the main habitat of chum salmon could move from the Bering Sea to the Western Arctic during summer.

This study is the first attempt to estimate the potential habitat for chum salmon in the Western Arctic using a bioenergetics model. Although we did not discuss the difference in the growth rate of chum salmon between the Bering Sea and the Western Arctic, this topic needs to be considered to clarify whether chum salmon migrate to the Western Arctic and if so when. Further modeling should be performed with a wide model domain including the Gulf of Alaska, the Bering Sea, and the Chukchi Sea using an individual-based model, which is a useful modeling tool to represent the behavior of individual fish, such as searching for a habitat (Tyler and Rose, 1994).

In the NPZD ecosystem model such as NEMURO, the top predator (ZP in our model: prey for chum salmon) usually includes all predators higher than predatory zooplankton. In our model, ZP biomass must include not only carnivorous zooplankton, but also the higher predators such as whales or salmon themselves. Therefore,

considering prey for chum salmon, future model developments should divide ZP into several categories. In addition, the conversion of model biomass units from nitrogen to wet weight needs to account for the difference in water content and nitrogen content between gelatinous zooplankton and crustacean zooplankton. Dividing ZP into several categories will be necessary to account for this in future model analyses. Moreover, global warming is associated with concurrent shifts in water temperature, salinity, sea level, fresh water input, stratification, circulation patterns, and so on in marine system (Harley et al., 2006; Doney et al., 2012; Yoon et al., 2013). Although we considered only water temperature used for the NEMURO formulations in the global warming scenario, responses of chum salmon migration to the other oceanographic conditions should be taken into account in future model developments. Furthermore, many salmon research cruises have been conducted in the Bering Sea, but the survey area should be expanded into the Chukchi Sea to respond to global warming.

Acknowledgements

This work was financially supported by the Ministry of Agriculture, Forestry and Fisheries, Japan through a research project entitled "Development of technologies for mitigation and adaptation to climate change in Agriculture, Forestry and Fisheries". E. Watanabe and M.J. Kishi were funded by the Grants-in-Aid for Scientific Research (S) of Japan Society for the Promotion of Science JFY2010–2014, No. 22221003, "Catastrophic reduction of sea ice in the Arctic Ocean: its impact on the marine ecosystems in the polar region". The 3-D NEMURO experiments were executed using Earth Simulator version 2 of Japan Agency for Marine-Science and Technology (JAMSTEC).

Appendix A: Formulations for the individual processes in the chum salmon bioenergetics model

Consumption rate (C) was estimated as the proportion of the maximum daily rations for chum salmon at a particular mass and temperature (Megrey et al., 2002; Beauchamp et al., 1989; Ito et al., 2004):

$$C = C_{MAX} \cdot \rho \cdot f_c(T) \tag{A.1}$$

$$C_{MAX} = \mathrm{ac} \cdot W^{\mathrm{bc}} \tag{A.2}$$

$$\rho = \frac{\frac{PD \cdot V_i}{K_i}}{1 + \frac{PD \cdot V_i}{K_i}} \tag{A.3}$$

where C_{MAX} is the maximum consumption rate (g prey g fish^{-1} d^{-1}), ρ is the available consumption rate without temperature effects, $f_c(T)$ is a temperature dependence function for consumption, T is water temperature (°C), ac is the intercept of the mass dependence function for a 1 g fish at the optimum water temperature, bc is the coefficient of the mass dependence, PD is the density of prey (g wet weight m^{-3} or g prey m^{-3}), V_i is the vulnerability at stage i (no dimension), and K_i is the half saturation constant (g prey m^{-3}).

Temperature dependence in the bioenergetics model, $f_c(T)$, is generally modeled as a dome-shaped curve as proposed by Thornton and Lessem (1978). The Thornton and Lessem function is the product of two sigmoid curves: one fits the increasing segment (gcta) and the other fits the decreasing segment (gctb) of the temperature dependence function:

$$f_c(T) = \mathrm{gcta} \cdot \mathrm{gctb} \tag{A.4}$$

(The increasing segment)

$$\mathrm{gcta} = \frac{(\mathrm{xk1} \cdot \mathrm{t4})}{(1.0 + \mathrm{xk1} \cdot (\mathrm{t4} - 1.0))} \tag{A.5}$$

$$\mathrm{t4} = e^{[\mathrm{t5} \cdot (T - \mathrm{te1})]} \tag{A.6}$$

$$\mathrm{t5} = \mathrm{tt5} \cdot \ln\left[0.98 \cdot \frac{(1.0 - \mathrm{xk1})}{(0.02 \cdot \mathrm{xk1})}\right] \tag{A.7}$$

$$\mathrm{tt5} = \frac{1}{(\mathrm{te2} - \mathrm{te1})} \tag{A.8}$$

(The decreasing segment)

$$\mathrm{gctb} = \frac{(\mathrm{xk4} \cdot \mathrm{t6})}{(1.0 + \mathrm{xk4} \cdot (\mathrm{t6} - 1.0))} \tag{A.9}$$

$$\mathrm{t6} = e^{[\mathrm{t7} \cdot (\mathrm{te4} - T)]} \tag{A.10}$$

$$\mathrm{t7} = \mathrm{tt7} \cdot \ln\left[0.98 \cdot \frac{(1.0 - \mathrm{xk4})}{(0.02 \cdot \mathrm{xk4})}\right] \tag{A.11}$$

$$\mathrm{tt7} = \frac{1}{(\mathrm{te4} - \mathrm{te3})} \tag{A.12}$$

where te1 and te2 are the lower and higher water temperatures in the increasing segment, in which the temperature dependence is the small fraction xk1 and the large fraction xk2 of the maximum consumption rate, respectively. te3 and te4 are the lower and higher water temperatures in the decreasing segment, in which the temperature dependence is the large fraction xk3 and the small fraction xk4 of the maximum consumption rate, respectively.

Respiration rate (R) was estimated as the amount of energy used for routine metabolism, and depends on body weight, ambient temperature, and activity (swimming speed) (Trudel et al., 2004; Ware, 1978):

$$R = (\mathrm{Rs} + \mathrm{Ra}) \cdot 5.258 \tag{A.13}$$

$$\mathrm{Rs} = \mathrm{ars} \cdot W^{\mathrm{br}} \cdot e^{(\mathrm{cr} \cdot T)} \tag{A.14}$$

$$\mathrm{Ra} = \mathrm{ara} \cdot W^{\mathrm{dr}} \cdot U^{\mathrm{er}} \tag{A.15}$$

$$\mathrm{ara} = (2.71 \times 10^{-4}) - (4.96 \times 10^{-6} \times T) + (5.63 \times 10^{-8} \times T^2) + (5.74 \times 10^{-7} \times S) - \left(7.72 \times 10^{-9} \times S^2\right) \tag{A.16}$$

$$U = \mathrm{au} \cdot W^{\mathrm{bu}} \tag{A.17}$$

where Rs is the standard metabolism (g O_2 g fish$^{-\mathrm{br}}$ d^{-1}), ars is the oxygen consumption rate of a 1 g fish at 0 °C (which depends on temperature), br is a coefficient relating the body weight to the standard metabolism, cr is a coefficient relating temperature to the standard metabolism, Ra is the activity metabolism when the fish moves (g O_2 g fish$^{-\mathrm{dr}}$ d^{-1}), ara is the oxygen consumption rate of 1 g fish at 0 °C which depends on activity, dr is a coefficient relating the body weight to the activity metabolism, er is a coefficient relating the swimming speed to the activity metabolism, S is salinity, U is the swimming speed (cm s^{-1}), au is the intercept of the mass dependence function for optimal foraging speed, and bu is a coefficient relating the body weight to the swimming speed. A coefficient of 5.258 in (A.13) is used to convert (g O_2 g fish^{-1} d^{-1}) into (g prey g fish^{-1} d^{-1}) (Megrey et al., 2002):

$$\left(\frac{13560\ \mathrm{J}}{1\ \mathrm{g\ O_2}} \times \frac{1\ \mathrm{cal}}{4.18\ \mathrm{J}}\right) \div \left(\frac{2580\ \mathrm{J}}{1\ \mathrm{g\ prey}} \times \frac{1\ \mathrm{cal}}{4.18\ \mathrm{J}}\right) = 5.258\ \mathrm{g\ prey\ g\ O_2^{-1}} \tag{A.18}$$

Kamezawa et al. (2007) changed the parameters reported in Trudel et al. (2004), but this was not mentioned in their paper. We used the same formulations and parameters reported in Kamezawa et al. (2007), thus we need to indicate the difference

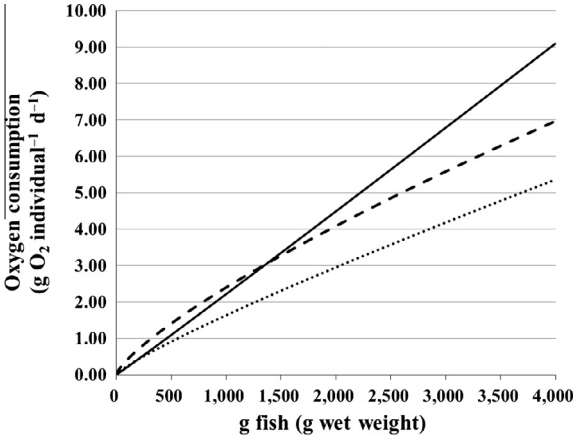

Fig. A.1. Relationship between the body weight and the oxygen consumption calculated using the formulations of Kamezawa et al. (2007) (for chum salmon; solid line), Trudel et al. (2004) (for sockeye salmon; dashed line), and Megrey et al. (2002) (for Pacific herring; dotted line).

in respiration between Kamezawa et al. (2007) and Trudel et al. (2004) as follows. Fig. A.1 shows the relationship between the body weight (g wet weight) and the oxygen consumption (g O_2 individual^{-1} d^{-1}), which were calculated using the formulations of Kamezawa et al. (2007) (for chum salmon; solid line), Trudel et al. (2004) (for Pacific salmon; dashed line), and Megrey et al. (2002) (for Pacific herring; dotted line). The oxygen consumption of Kamezawa et al. (2007) is lower for fish below 1350 g, but higher for fish above 1350 g than the values used in Trudel et al. (2004), and the difference becomes larger as the body weight increases.

Specific dynamic action (SDA) and excretion (E, nitrogenous waste) were estimated as a proportion of assimilated energy, and egestion (F, fecal waste) was estimated as a proportion of consumption (Megrey et al., 2002):

$$\mathrm{SDA} = \mathrm{ss} \cdot (C - F) \tag{A.19}$$

$$F = \mathrm{af} \cdot C \tag{A.20}$$

$$E = \mathrm{ae} \cdot (C - F) \tag{A.21}$$

where ss is the coefficient for specific dynamic action, and af and ae are the constant proportions of consumed food that are egested and excreted, respectively.

References

Aita, M.N., Yamanaka, Y., Kishi, M.J., 2007. Interdecadal variation of the lower trophic ecosystem in the northern Pacific between 1948 and 2002, in a 3-D implementation of the NEMURO model. Ecological Modelling 202, 81–94.

Azumaya, T., Ishida, Y., 2004. An evaluation of the potential influence of SST and currents on the oceanic migration of juvenile and immature chum salmon (*Oncorhynchus keta*) by a simulation model. Fisheries Oceanography 13, 10–23.

Azumaya, T., Ishida, Y., 2005. Mechanism of body cavity temperature regulation of chum salmon (*Oncorhynchus keta*) during homing migration in the North Pacific Ocean. Fisheries Oceanography 14, 81–96.

Beauchamp, D.A., Stewart, D.J., Thomas, G.L., 1989. Corroboration of a bioenergetics model for sockeye salmon. Transactions of the American Fisheries Society 118, 597–607.

Campbell, R.G., Sherr, E.B., Ashjian, C.J., Plourde, S., Sherr, B.F., Hill, V., Stockwell, D.A., 2009. Mesozooplankton prey preference and grazing impact in the western Arctic Ocean. Deep-Sea Research II 56, 1274–1289.

Cook, M.E.A., Sturdevant, M.V., 2013. Diet composition and feeding behavior of juvenile salmonids collected in the northern Bering Sea. North Pacific Anadromous Fish Commission Technical Report 9, 118–126.

Doney, S.C., Ruckelshaus, M., Duffy, J.E., Barry, J.P., Chan, F., English, C.A., Galindo, H.M., Knowlton, N., Polovina, J., Rabalais, N.N., Sydeman, W.J., Talley, L.D., 2012. Climate change impacts on marine ecosystems. Annual Review of Marine Science 4, 11–37.

Echave, K., Eagleton, M., Farley, E., Orsi, J., 2012. A refined description of essential fish habitat for Pacific salmon with the U.S. Exclusive Economic Zone in Alaska. U.S. Dep. Commer., NOAA Tech. Memo. NMFS-AFSC-236, 104 p.

Hanson, P.C., Johnson, T.B., Schindler, D.E., Kitchell, J.F., 1997. Fish bioenergetics 3.0 for Windows. University of Wisconsin Sea Grant Institute Technical Report, Madison, WI, USA.

Harley, C.D.G., Hughes, A.R., Hultgren, K.M., Miner, B.G., Sorte, C.J.B., Thornber, C.S., Rodriguez, L.F., Tomanke, L., Williams, S.L., 2006. The impacts of climate change in coastal marine systems. Ecology Letters 9, 228–241.

Hasumi, H., 2006. CCSR Ocean Component Model (COCO) version 4.0. Center for Climate System Research, Tokyo, University of Tokyo, Tokyo, Japan.

Hasumi, H., Emori, S., 2004. K-1 Coupled GCM (MIROC) Description. Center for Climate System Research, University of Tokyo, Tokyo, Japan.

Hopcroft, R.R., Kosobokova, K.N., Pinchuk, A.I., 2010. Zooplankton community patterns in the Chukchi Sea during summer 2004. Deep-Sea Research II 57, 27–39.

Ishida, Y., Yano, A., Ban, M., Ogura, M., 2001. Vertical movement of a chum salmon *Oncorhynchus keta* in the western North Pacific Ocean as determined by a depth-recording archival tag. Fisheries Science 67, 1030–1035.

Ito, S., Kishi, M.J., Kurita, Y., Oozeki, Y., Yamanaka, Y., Megrey, B.A., Werner, F.E., 2004. Initial design for a fish bioenergetics model of Pacific saury coupled to a lower trophic ecosystem model. Fisheries Oceanography 13, 111–124.

Kaeriyama, M., 2008. Ecosystem-based sustainable conservation and management of Pacific salmon. In: Tsukamoto, K., Kawamura, T., Takeuchi, T., Beard, T.D., Kaiser, M.J. (Eds.), Fisheries for Global Welfare and Environment. 5th World Fisheries Congress 2008, Terra Scientific Publishing Company, Tokyo, Japan, pp. 371–380.

Kaeriyama, M., Nakamura, M., Edpalina, R., Bower, J.R., Yamaguchi, H., Walker, R.V., Myers, K.W., 2004. Change in feeding ecology and trophic dynamics of Pacific salmon (*Oncorhynchus* spp.) in the central Gulf of Alaska in relation to climate events. Fisheries Oceanography 13, 197–207.

Kaeriyama, M., Seo, H., Kudo, H., Nagata, M., 2012. Perspectives on wild and hatchery salmon interactions at sea, potential climate effects on Japanese chum salmon, and the need for sustainable salmon fishery management reform in Japan. Environmental Biology of Fishes 94, 165–177.

Kamezawa, M., Azumaya, T., Nagasawa, T., Kishi, M.J., 2007. A fish bioenergetics model of Japanese chum salmon (*Oncorhynchus keta*) for studying the influence of environmental factor changes. Bulletin of the Japanese Society of Fisheries Oceanography 71, 87–95 (in Japanese, with English Abstr.).

Kawamiya, M., Yoshikawa, C., Kato, T., Sato, H., Sudo, K., Watanabe, S., Matsuno, T., 2005. Development of an integrated earth system model on the earth simulator. Journal of the Earth Simulator 4, 18–30.

Kishi, M.J., Kaeriyama, M., Ueno, H., Kamezawa, Y., 2010. The effect of climate change on the growth of Japanese chum salmon (*Oncorhynchus keta*) using a bioenergetics model coupled with a three-dimensional lower trophic ecosystem model (NEMURO). Deep-Sea Research II 57, 1257–1265.

Kishi, J.M., Kashiwai, M., Ware, D.M., Megrey, B.A., Eslinger, D.L., Werner, F.E., Aita, M.N., Azumaya, T., Fujii, M., Hashimoto, S., Huang, D., Iizumi, H., Ishida, Y., Kang, S., Kantakov, G.A., Kim, H., Komatsu, K., Navrotsky, V.V., Smith, S.L., Tadokoro, K., Tsuda, A., Yamamura, O., Yamanaka, Y., Yokouchi, K., Yoshie, N., Zhang, J., Zuenko, Y.I., Zvalinsky, V.I., 2007. NEMURO—a lower trophic level model for the North Pacific marine ecosystem. Ecological Modelling 202, 12–25.

Locarnini, R.A., Mishonov, A.V., Antonov, J.I., Boyer, T.P., Garcia, H.E., 2006. World Ocean Atlas 2005, Volume 1: Temperature. In: Levitus, S. (Ed.), NOAA Atlas NESDIS 61. U.S. Government Printing Office, Washington, D.C., USA, p. 182.

Megrey, B.A., Rose, K.A., Werner, F.E., Klumb, R.A., Hay, D., 2002. A generalized fish bioenergetics/biomass model with an application to Pacific herring. PICES Scientific Report 20, 4–12.

Morita, K., Sato, S., Kato, M., Yamamoto, J., 2009. The summer 2009 Japanese salmon research cruise of the R/V Hokko maru: exploration of the northern limit of offshore distribution and annual survey in the Bering sea. North Pacific Anadromous Fish Commission Documents 1191, 12 pp.

Moss, J.H., Murphy, J.M., Farley, E.V., Eisner, L.B., Andrews, A.G., 2009. Juvenile pink and chum salmon distribution, diet, and growth in the northern Bering and Chukchi seas. North Pacific Anadromous Fish Commission Bulletin 5, 191–196.

Nagasawa, T., Azumaya, T., 2009. Distribution and CPUE trends in Pacific salmon, especially sockeye salmon in the Bering Sea and adjacent waters from 1972 to the mid 2000s. North Pacific Anadromous Fish Commission Bulletin 5, 1–13.

Neave, F., Yonemori, T., Bakkala, R.G., 1976. Distribution and origin of chum salmon in offshore waters of the North Pacific Ocean. International North Pacific Fisheries Commission Bulletin 35, 1–79.

Orsi, J.A., Wertheimer, A.C., Sturdevant, M.V., Fergusson, E.A., Mortensen, D.G., Wing, B.L., 2004. Juvenile chum salmon consumption of zooplankton in marine waters of southeastern Alaska: a bioenergetics approach to implications of hatchery stock interactions. Review in Fish Biology and Fisheries 14, 335–359.

Perry, R.I., Hargreaves, N.B., Waddell, B.J., Mackas, D.L., 1996. Spatial variations in feeding and condition of juvenile pink and chum salmon off Vancouver Island, British Columbia. Fisheries Oceanography 5, 73–88.

Rudstam, L.G., 1988. Exploring the dynamics of herring consumption in the Baltic: Applications of an energetic model of fish growth. Kieler Meeresforsch. Sonderh. 6, 312–322.

Sato, S., Kato, M., Morita, K., Urawa, S., 2012. Stock-specific summertime distribution of immature chum salmon in the Bering Sea as inferred from SNP markers. North Pacific Anadromous Fish Commission Technical Report 8, 50–51.

Sato, S., Moriya, S., Azumaya, T., Nagoya, H., Abe, S., Urawa, S., 2009a. Stock distribution patterns of chum salmon in the Bering Sea and North Pacific Ocean during the summer and fall of 2002–2004. North Pacific Anadromous Fish Commission Bulletin 5, 29–37.

Sato, S., Takahashi, M., Watanabe, N., Kitatsuji, S., Takasaki, D., Chiba, T., Imai, S., Goda, Y., Katayama, Y., Kagaya, M., Fukuwaka, M., Agler, B.A., Urawa, S., 2009b. Preliminary records of otolith-marked chum salmon found in the Bering Sea and North Pacific Ocean in 2006 and 2007. North Pacific Anadromous Fish Commission Bulletin 5, 99–104.

Sherr, E.B., Sherr, B.F., Hartz, A.J., 2009. Microzooplankton grazing impact in the Western Arctic Ocean. Deep-Sea Research II 56, 1264–1273.

Steele, M., Ermold, W., Zhang, J., 2008. Arctic Ocean surface warming trends over the past 100 years. Geophysical Research Letters 35, L02614. http://dx.doi.org/10.1029/2007GL031651.

Tadokoro, K., Ishida, Y., Davis, N.D., Ueyanagi, S., Sugimoto, T., 1996. Change in chum salmon (*Oncorhynchus keta*) stomach contents associated with fluctuation of pink salmon (*O. gorhuscha*) abundance in the central subarctic Pacific and Bering Sea. Fisheries Oceanography 5, 89–99.

Thornton, K.W., Lessem, A.S., 1978. A temperature algorithm for modifying biological rates. Transactions of the American Fisheries Society 107, 284–287.

Trudel, M., Geist, D.R., Welch, D.W., 2004. Modeling the oxygen consumption rates in Pacific salmon and steelhead: an assessment of current models and practices. Transactions of the American Fisheries Society 133, 326–348.

Tyler, J.A., Rose, A.R., 1994. Individual variability and spatial heterogeneity in fish population models. Reviews in Fish Biology and Fisheries 4, 91–123.

Urawa, S., 2000. Ocean migration route of Japanese chum salmon with a reference to future salmon research. National Salmon Resources Center Newsletter 5, 3–9 (in Japanese).

Urawa, S., Sato, S., Crane, P.A., Agler, B., Josephson, R., Azumaya, T., 2009. Stock-specific ocean distribution and migration of chum salmon in the Bering Sea and North Pacific Ocean. North Pacific Anadromous Fish Commission Bulletin 5, 131–146.

Walker, R.V., Myers, K.W., Davis, N.D., Aydin, K.Y., Friedland, K.D., Carlson, H.R., Boehlert, G.W., Urawa, S., Ueno, Y., Anma, G., 2000. Diurnal variation in thermal environment experienced by salmonids in the North Pacific as indicated by data storage tags. Fisheries Oceanography 9, 171–186.

Ware, D.M., 1978. Bioenergetics of pelagic fish: theoretical change in swimming speed and ration with body size. Journal of the Fisheries Research Board of Canada 35, 220–228.

Watanabe, E., 2011. Beaufort shelf break eddies and shelf-basin exchange of Pacific summer water in the western Arctic Ocean detected by satellite and modeling analyses. Journal of Geophysical Research 116, C08034. http://dx.doi.org/10.1029/2010JC006259.

Watanabe, E., Hasumi, H., 2009. Pacific water transport in the western Arctic Ocean simulated by an eddy-resolving coupled sea ice-ocean model. Journal of Physical Oceanography 39, 2194–2211.

Watanabe, E., Kishi, M.J., Ishida, A., Aita, M.N., 2012. Western Arctic primary productivity regulated by shelf-break warm eddies. Journal of Oceanography 68, 703–718.

Watanabe, E., Onodera, J., Harada, N., Honda, N.C., Kimoto, K., Kikuchi, T., Nishino, S., Matsuno, K., Yamaguchi, A., Ishida, A., Kishi, M.J., 2014. Enhanced role of eddies in the Arctic marine biological pump. Nature Communications 5, 3950. http://dx.doi.org/10.1038/ncomms4950.

Yoon, S., Abe, H., Kishi, M.J., 2013. Responses of Manila clam growth and its food sources to global warming in a subarctic lagoon in Japan. Progress in Oceanography 119, 48–58.